Radioimmunodetection of Medullary Thyroid Cancer Using a Bispecific Anti-CEA/ Anti-Indium-DTPA Antibody and an Indium-111-Labeled DTPA Dimer

Patrick Peltier, Chantal Curtet, Jean-François Chatal, Jean-Marc Le Doussal, Georges Daniel, Geneviève Aillet, Anne Gruaz-Guyon, Jacques Barbet and Michel Delaage

Nuclear Medicine Department, Centre Rene Gauducheau, Nantes, France; INSERM U211, Nantes, France; Immunotech SA, Marseille, France; DAMRI, Saclay, France; Anatomopatology Department, Nantes, France; and Pasteur Institut, Lille, France

Two-step radioimmunotargeting using a bispecific anti-CEA/anti-In-DTPA monoclonal antibody and an ^{111}In-labeled DTPA dimer (diDTPA-TL) was evaluated nine times in eight patients with medullary thyroid cancer (MTC). Immunoscintigraphy was performed 5 and 24 hr after injection of ^{111}In-diDTPA-TL. For five patients, radioimmunoguided surgery (RIGS) was performed using a hand-held gamma probe (sodium iodine), and a biodistribution study was performed 48 hr (four times) and 24 hr (one time) after injection of ^{111}In-diDTPA-TL. Mean tumor uptake (%ID/kg in tumor) was 39 (range 2.75–139). In these five patients, immunoscintigraphy visualized all known tumors and detected unknown foci (US and CT were negative) in the neck (once) and neck and liver (once). Immunoscintigraphy, performed four times in search of a recurrence, detected unknown localizations in the mediastinum and neck (twice) and was negative twice. There were no false-positives. In three of five patients who had surgery, RIGS localized tumor foci not detected by the surgeon. RIGS failed to detect two small lesions (10 × 10 mm) corresponding to sites of fibrosis and microscopic cancer infiltration. Bispecific anti-CEA/anti-In-DTPA mediated targeting of ^{111}In-diDTPA-TL provided elevated tumor uptake and tumor-to-normal tissue ratios. Radioimmunodetection of small MTC lesions is thus possible even when morphological imaging techniques prove negative.

J Nucl Med 1993; 34:1267–1273

During monitoring of medullary thyroid cancer (MTC), a rise in serum concentration of thyrocalcitonin (TCT) and/or carcinoembryonic antigen (CEA) is suggestive of tumor recurrence. Morphological imaging techniques [ultrasonography (US), computed tomography (CT), magnetic resonance imaging (MRI)] can confirm and localize a biologically detected recurrence but are sometimes inadequate because of topographic polymorphism (neck, mediastinum, lung, liver, bone) and the small size of tumor recurrences at an early stage of development (*1–3*). The existence of fibrous modifications after neck surgery and a tumor density similar to that of normal tissues can also affect the diagnostic accuracy of these techniques. In nuclear medicine, various examinations have been proposed (^{201}Tl, MIBG, pentavalent DMSA), but none has proved sufficiently reliable (*4–10*). Another possibility is the use of ^{131}I-labeled anti-TCT monoclonal antibodies, but initial results have not been confirmed by clinical studies (*11–13*). CEA is present at the cell surface of MTC, which frequently expresses it (*14–16*), whereas TCT is expressed essentially in cell cytoplasm (*14*). Promising results have been obtained with ^{131}I- and ^{111}In-labeled anti-CEA monoclonal antibodies (*17–23*). Because tumor-to-normal tissue ratios are sometime moderate with the direct labeling technique, a two-step radioimmunotargeting technique has been developed (*24,25*). A preliminary clinical study performed for primary colon cancers indicates that relative background intensity can be reduced by a factor of 4 to 5 (*26*). This technique, requiring subsequent injections of a bispecific anti-CEA/anti-IN-DTPA monoclonal antibody and of a ^{111}In-labeled DTPA dimer, was evaluated in the present study for radioimmunodetection, including immunoscintigraphy and radioimmunoguided-surgery (RIGS), of MTC.

METHODS

Patients

Eight patients with MTC (4 men, 4 women; mean age 50 yr) gave informed consent to participate in the study. Patient data are given in Table 1. Immunoscintigraphy and RIGS were performed on Patients 2 and 3 who had had surgery for primary tumors and on Patients 1, 7 and 8 who had surgery for known tumor recurrence. The latter patients had MTC for a mean period of 14 mo. TCT concentration was elevated (1235, 1700 and 6500 ng/liter; n <

Received Jul. 7, 1992; revision accepted Apr. 13, 1993.

For correspondence or reprints contact: Patrick Peltier, MD, Service de Médecine Nucléaire, Hotel Dieu, CHU de Nantes, place Ricordeau, 44035 Nantes Cedex 01, France.

TABLE 1
Patient Data

Patient no.	Type	US	CT	TCT/CEA	Immunoscintigraphy	Diagnosis
1	B	Neck (−)	Neck (−) Thorax (−)	1235/3*	Neck (+) Thorax (−)	Neck (+), surgery Thorax (−), course (6 mo)
2	A	Neck (+)	Thorax (−)	4870/540*	Neck (+) Thorax (−)	Neck (+), surgery Thorax (−), course (6 mo)
3	A	Neck (+)	Thorax (−)	1383/290*	Neck (+) Thorax (−)	Neck (+), surgery Thorax (−), course (6 mo)
4	C	Neck (−)	Neck (−) Thorax (−)	61/5*	Neck (−) Thorax (−)	Neck (−), course (6 mo) Thorax (−), course (6 mo)
5	C	Neck (−)	Neck (−) Thorax (−)	25/3*	Neck (−) Thorax (±)	Neck (−), course (6 mo) Thorax (−), course (6 mo)
6	D	Neck (−)	Thorax (+)	281/10†	Neck (+) Thorax (+)	Neck (+), course (1 mo) Thorax (+), course (1 mo)
7a	C	Neck (−)	ND	1676/12†	Neck (+) Thorax (+)	Neck (+), surgery Thorax (+), surgery
7b	B	Neck (+)	Neck (+) Thorax (+)	1700/10†	Neck (+) Thorax (+)	
8	B	Neck (±)	Neck (±) Thorax (−) Liver (−)	6506/22*	Neck (+) Thorax (−) Liver (+)	Neck (+), surgery Thorax (−), surgery Liver (+), course (1 mo)

*CEA normal value <6 ng/ml (ELSA2 CEA, Cis biointernational).
†CEA normal value ≤10 ng/ml (INX CEA, MEIA, Abbott).
Type: A = preoperative primary tumor, B = preoperative recurrence, C = search for recurrence, D = assessment of recurrence spread. Course = clinical and paraclinical (US and CT).

10 ng/liter) and CEA was elevated once (22 ng/ml), at the upper limit of normal once (10 ng/ml) and was normal once (3 ng/ml).

Immunoscintigraphy was performed on Patients 4, 5 and 7 because of biologically suspected recurrences indicated by an increase in serum markers (TCT with or without CEA). TCT concentration was moderately elevated twice (25 and 61 ng/liter) and markedly elevated once (1676 ng/liter), whereas CEA was normal twice (5 and 3 ng/ml) and at the upper limit of normal once (12 ng/ml). Patient 6 also received immunoscintigraphy to determined the spread of known metastases. The primary tumor had been surgically removed 1.5 mo previously. TCT concentration was elevated (281 ng/liter), whereas CEA was at the upper limit of normal (10 ng/ml).

Two-step Procedure

The bispecific antibody was composed of an Fab' fragment of anti-CEA monoclonal IgG1 (F6) (*22*) coupled chemically with the Fab fragment of anti-In-DTPA monoclonal IgG1 (734) (*24*). The tracer was an ^{111}In-labeled DTPA dimer (n-α-DTPA-tyrosyl-n-ε-DTPA-lysine(diDTPA-TL)). A mean quantity of 259 MBq (7 mCi) of ^{111}In-Cl3 (Cis biointernational, Gif/Yvette, France) was used to label diDTPA-TL.

Tumor radioimmunotargeting was performed in two steps. First, 1 mg/10 kg of nonradiolabeled bispecific antibody was injected by slow intravenous infusion (20 min). After an interval of 4 days, 1 nmol/10 kg of ^{111}In-labeled diDTPA-TL was injected.

To provide anatomical landmarks, 185 MBq (5 mCi) of ^{99m}Tc hydroxy-methylene-diphosphonate (HMDP) and albumin labeled with 74 MBq (2 mCi) of ^{99m}Tc were injected in all patients 4 hr after ^{111}In-diDTPA-TL.

A 10-ml blood sample was taken immediately before injection of the bispecific antibody for assay of serum markers (TCT, CEA) and HAMA. Clinical tolerance to the two injections (bispecific antibody and ^{111}In-diDTPA-TL) was monitored for 48 hr.

Immunoscintigraphy

Recordings were performed 5 and 24 hr after injection of ^{111}In-diDTPA-TL. Each included a whole-body scan and emission computed tomography (ECT), with spectrophotometric settings on the two ^{111}In photopeaks (173 and 247 keV). Anterior and posterior views were obtained using a gamma camera with two rectangular heads (DHD Sophy Camera, Sopha Médical, Buc, France) equipped with medium-energy collimators. The scanning speed was 12 cm/min. ECT was obtained by double-isotope acquisition: ^{111}In (173 and 247 keV) and ^{99m}Tc (140 keV). A large-field gamma camera (Sophy Camera; Sopha Médical) equipped with a medium-energy collimator recorded 64 projections (64 × 64 matrix) for 40 min in a step-by-step mode and 360° rotation. Six-millimeter sections were reconstructed in three planes (sagittal, frontal, transverse) using a Wiener filter.

Immunoscintigraphy images were interpreted blindly relative to surgery and follow-up. Whole-body scans and ECT were considered positive when a hot spot was sufficiently contrasted relative to surrounding structures.

Other Imaging Techniques

Cervical US (nine times) and thoracic and hepatic CT (eight times) were performed in the month preceding radioimmunodetection (Table 1). Cervical US and thoracic CT (Patient 7a) and

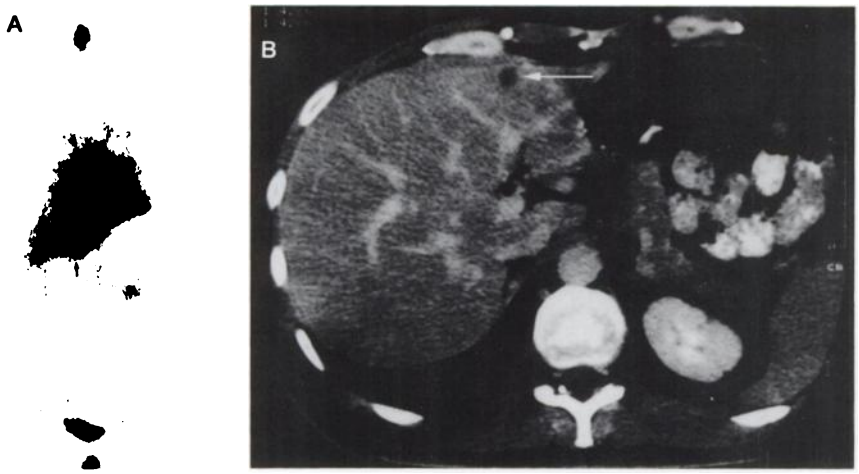

FIGURE 1. Patient 8. Anterior view (A) of the body scan recorded 5 hr after ^{111}In-diDTPA-TL injection clearly shows liver recurrence (arrow) not visualized by a previous CT scan. A second CT scan performed after immunoscintigraphy (B) confirmed a 10 × 10-mm recurrence (arrow).

hepatic CT (Patient 8) were performed subsequently to immunoscintigraphy. Cervical MRI was done for Patient 1.

RIGS and Biodistribution Study

RIGS and a biodistribution study were performed 48 hr (Patients 1, 2, 3, 7b) and 24 hr (Patient 8) after injection of ^{111}In-diDTPA-TL.

RIGS. A hand-held gamma probe with an electronic unit (MODELO 2 Localization Monitor; Oris/Damri, Gif sur Yvette, France) was used during surgery to count the activity at different sites in the operating field. The probe, housed in a stainless steel waterproof container (total length 200 mm), contains a 5-mm diameter, 15 mm long sodium iodide (NaI) scintillator and a photomultiplier. The electronic unit includes a microprocessor for pre-time or pre-count acquisition. Measurements were performed in the areas where a tumor was suspected and for lymph nodes, large vessels and muscles. Each measurement, expressed in counts per second (cps), was obtained at a pre-time of 10 sec, with the channel set for the 173 and 247 keV photopeaks of ^{111}In.

The utility of the detection probe was also evaluated qualitatively by asking the surgeon whether it facilitated detection of cancer sites not identifiable visually or by palpation and whether it led to a modification of the surgical act, i.e., the excision of lesions which otherwise would not have been resected.

Biodistribution. Fragments of tumor, lymph nodes and muscle removed by the surgeon and a blood sample were weighed and then counted in a gamma well counter. Results were expressed as a percentage of injected dose per kilogram of tissue (%ID/kg). The tumor fragments were immediately immersed in formol (10%) for paraffin embedding and immunohistochemical study.

CEA distribution was assessed by immunoperoxidase staining of the paraffin-embedded sections using the same CEA antibody and the avidin-biotin method. Staining intensity was determined by a semiquantitative method in which +++ was strong staining, ++ medium staining and + weak staining. The percentage of cancer cells in tumor was estimated for each section.

Human anti-bispecific-monoclonal antibody concentration was determined in duplicate from serum (100 μl, final solution 1/3) using a one-step sandwich radioimmunoassay with F6-734 bispecific monoclonal antibody on the solid phase and ^{125}I-labeled F6-734 bispecific monoclonal antibody as tracer.

RESULTS

Human antimouse assay (HAMA) screening of the blood sample obtained just before the bispecific antibody injection was negative eight times. HAMA were detected in Patient 7 in the sample obtained just before the second bispecific antibody injection, whereas screening 10 days before (i.e., 40 days after the first injection) had been negative. No signs of intolerance were observed in any of the patients (including Patient 7b) within 48 hr after bispecific antibody or ^{111}In-diDTPA-TL injection.

Imaging Results

Whole-body Scan and ECT Data. Qualitative (visual) interpretation of the body scan images obtained 5 hr after injection of ^{111}In-diDTPA-TL showed marked blood-pool activity (heart and vessels) associated with renal, hepatic, vesical and scrotal activity. Pathological hot spots were clearly distinct, including those in the liver (Fig. 1) and mediastinum.

In images recorded at 24 hr, as compared to those at 5 hr, the relative intensity of vascular activity had markedly decreased, whereas that of the kidneys, bladder and scrotum showed no change and that of the liver was increased. Pathological hot spots were better contrasted relative to surrounding nonspecific activity (Fig. 2).

No bone marrow uptake was detected at these two recording times. At both times, the patient with HAMA (No. 7b) had much lower vascular activity, much higher hepatic activity and reduced tumor activity, but with an apparent increase in tumor-to-blood contrast (Fig. 3).

The whole-body scan and ECT images gave the same results in all patients except No. 5 (Table 1). In this patient, the whole-body scan showed no pathological focus, whereas the different ECT sections indicated bilateral thoracic and right cervicomediastinal junction abnormalities. The weak contrast of these foci did not clearly indicate the presence of cancer recurrences.

Analysis of Patient Results. Immunoscintigraphy was performed three times to search for tumor recurrences strongly suggested by a rise in TCT concentration when morphological imaging techniques (US, CT) were negative. In Patient 7a, immunoscintigraphy detected neck (negative US) and mediastinal (CT not done) foci. A second cervical US and thoracic CT performed after immunoscintigraphy visualized these foci, which were surgically confirmed 2

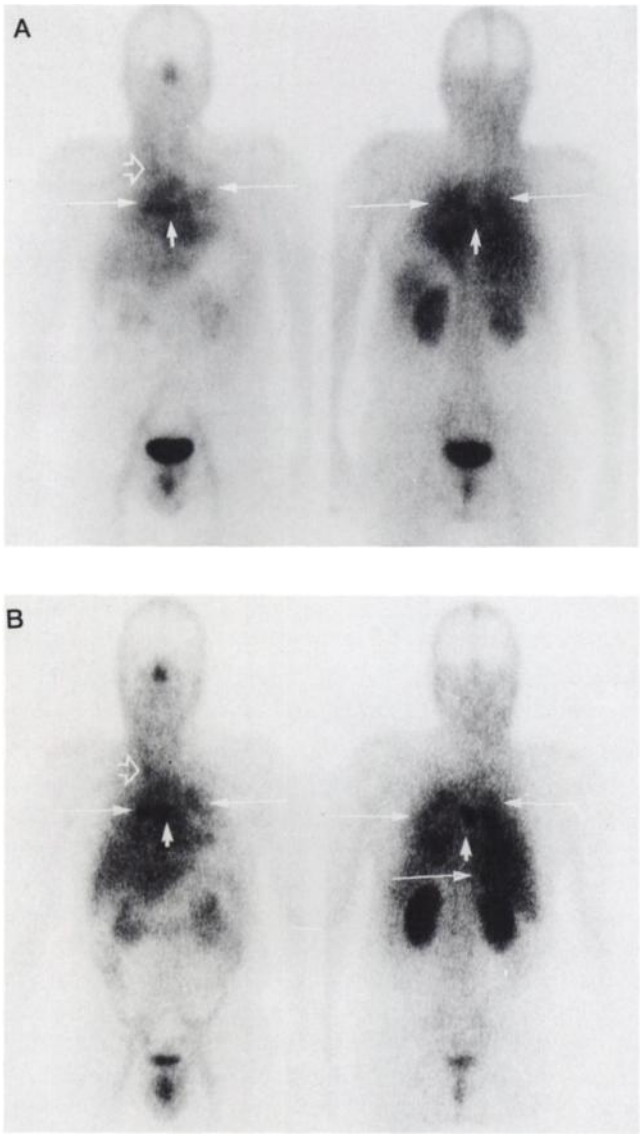

FIGURE 2. Patient 6. Body scan recorded 5 hr (A) and 24 hr (B) after ^{111}In-diDTPA-TL injection. Although blood-pool activity slightly hinders recurrence imaging, mediastinal (short arrow), lung (long arrow) and cervical (open arrow) recurrences are shown (A). (B) Recurrences, decreased blood-pool activity and relatively liver activity increased.

mo later. The first focus corresponded to a 15 × 5-mm jugulocarotid lymph node and the second to four brachiocephalic trunk lymph nodes measuring on average 10 × 10 mm. In Patient 4, immunoscintigraphy was negative (negative US and CT), and no recurrence had been confirmed after 6 mo of follow-up. In Patient 5, ECT showed nonsignificant thoracic spots (low activity), whereas the whole-body scan, US and CT were normal. ECT spots could have been due to breast or vessel activity.

Immunoscintigraphy was performed three times just before surgery for a previously diagnosed recurrence. In two of these patients (Nos. 1 and 8), the recurrence had been detected 3 and 4 mo earlier by immunoscintigraphy after injection of the same anti-CEA monoclonal antibody in F(ab')$_2$ fragment form directly labeled with ^{111}In. The results of ^{111}In-F6 and two-step radioimmunotargeting (anti-CEA/anti-In-DTPA and ^{111}In-diDTPA-TL) could thus be compared. In both cases, after injection of ^{111}In-F6, tumor contrast was moderate with respect to vessels and especially liver so that clear visualization of tumor lesions was only possible after image processing. In Patient 1, ^{111}In-F6 visualized one neck lesion, whereas two-step radioimmunotargeting showed two cervical foci which were confirmed by surgery (9 × 10 mm and 16 × 10 mm) (Fig. 4). These cervical lesions were not detected by US, CT and MRI. In Patient 8, ^{111}In-F6 barely visualized a cervical focus and a mediastinal focus, whereas two-step radioimmunotargeting clearly showed only the cervical focus. Cervicotomy confirmed the neck lesion (7 × 10 mm), and no mediastinal tumor was found in thoracotomy. Moreover, for this same patient, two-step radioimmunotargeting revealed a pathological hepatic focus that had not been visu-

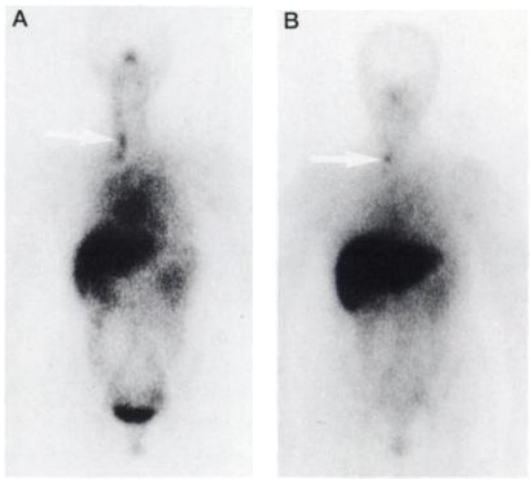

FIGURE 3. Patient 7. Anterior view of body scan of Patient (A, first injection) and (B, second injection) recorded 24 hr after ^{111}In-diDTPA-TL injection. (A) Cervico-mediastinal recurrences (arrow). (B) Same recurrence (arrow) without image processing. However, due to increased liver activity, lesions were less visible. HAMA presence probably accounts for the higher liver and lower recurrence activity when compared to (A). Blood-pool activity is also decreased in (B) and tumor-to-blood contrast has apparently increased.

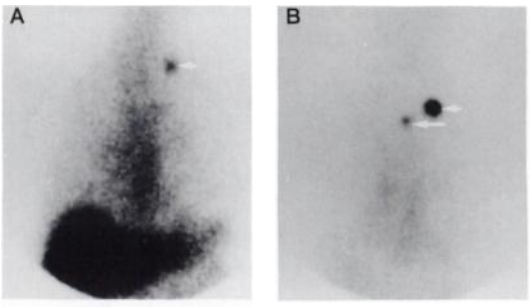

FIGURE 4. Patient 1. Planar scan recorded 3 days after injection of anti-CEA (F6) directly labeled with ^{111}In (A). Planar scan recorded 24 hr after ^{111}In-diDTPA-TL injection (B). Intense hepatic and blood-pool activity and a left neck recurrence (arrow) are seen (A). Same neck recurrence (short arrow) as well as a second one (long arrow) (B). Liver and blood-pool activity are lower than that of tumor hot spots.

TABLE 2
RIGS Results

Patient no.	Type	Size	T-to-Blood	T-to-Muscle	T-to-nLyN
1	LyN 1	9*10	4.5	2.8	2.5
	LyN 2	16*10	8.9	5.5	4.9
2	pt	40*30	1.4	2.6	1.9
3	pt	30*30	5.2	5.9	4.5
	LyN	10*10	0.8	0.9	0.7
7b	LyN 1	50*26	2.6	3.7	4
	LyN 2	15*5	1.2	1.7	1.8
8	LyN 1	7*10	1.5	2.1	1.7
	LyN 2	10*10	0.8	1	0.9

Type = Tumor type; LyN = lymph node; pt = primary tumor; size = tumor size in mm; T-to-blood, T-to-muscle and T-to-nLyN = tumor-to-blood, muscle and normal lymph node count ratios.

alized by CT. A second hepatic CT scan obtained after two-step radioimmunotargeting examination confirmed the presence of a 10-mm diameter recurrence in the left lobe of the liver (Fig. 4). The recurrence in patient 7b had been diagnosed by immunoscintigraphy with two-step radioimmunotargeting 2 mo before.

Two primary tumors (Patients 2 and 3) were visualized by immunoscintigraphy, but no other pathological cervical, thoracic or hepatic foci were detected in these patients by this technique. Patient 3, however, presented with a nodular micrometastasis (~2 mm in diameter) which was not detected by US and CT.

Immunoscintigraphy was performed once to study the spread of known lung metastases (Patient 6). Lung lesions previously visualized by CT were detected, as well as mediastinal and cervicomediastinal foci which had not been visualized by CT. These lesions were confirmed by further morphological examinations (US and CT) after immunoscintigraphy results had been obtained.

RIGS

Counting Values. The results for intraoperative counts performed in five patients are shown in Table 2. For tumor, the mean count rate was 1,700 cps (range 630–3400), whereas for normal lymph nodes (21 lymph nodes tested) it was 404 cps (range 280–460), for blood 610 (range 260–1270) and for muscle 400 cps (range 150–880). Among the nine tumors, the tumor-to-blood (mean 3, range 0.8–8.9), tumor-to-normal lymph node (mean 2.5, range 0.7–4.9) and tumor-to-muscle (mean 2.90 range 0.9–5.5) count ratios were higher than 1.5, respectively, five, seven and seven times. The two tumors for which tumor-to-normal lymph nodes and tumor-to-muscle count ratios were below 1.5 corresponded to micrometases less than 5 mm infiltrating lymph nodes (LyN in Patient 3 and LyN2 in Patient 8).

Surgical Usefulness. For the two patients (No. 2 and 3) who had surgery for a primary tumor, the NaI probe provided no additional information for the surgeon and did not modify his approach. The primary tumors were easily distinguished by the surgeon, and, for Patient 3, the probe failed to detect the microscopic malignant nodal infiltration discovered upon histological examination of the systematic radical neck nodal dissection.

For the three patients who had surgery for tumor recurrence, the NaI probe enabled the surgeon to differentiate five of six involved lymph nodes (tumor-to-muscle ratio >1.5) from uninvolved ones, whereas visual and palpatory surgical exploration was negative. Because of the NaI probe, tumor excision could be performed in two patients (Nos. 1 and 8). In Patient 1, recurrences smaller than 20 × 10 mm were found in the scar area from the previous operation. In Patient 8, a right submandibular recurrence was concealed in fibrous tissue, which could not have been detected by the surgeon. The second lymph node (midjugular region) was accessible and systematic neck nodal dissection was performed. For Patient 7b, however, the surgical approach was not modified by the use of the NaI probe since systematic excision of the involved lymph nodes in the neck and brachiocephalic trunk had been decided beforehand on the basis of immunoscintigraphic data.

Biodistribution

Tumor uptake was variable from patient to patient (2.7%–139% ID/kg) and from lesion to lesion in the same patient (Table 3). Tumor uptake concentration was elevated (>30% ID/kg) when antigenic expression was high (++ or +++ immunohistochemically) and the percentage of cancer cells in the tumor was greater than 70% (LyN1 in Patient 8, LyN1 and LyN2 in Patient 1). Conversely, tumor uptake was less elevated (7%–22% ID/kg) when antigenic expression was low (+) or the percentage of cancer cells was less than 70% (pt in Patient 3, LyN1 and LyN2 in Patient 7b).

Uptake was less than 5% ID/kg in three tumors: Lymph node 2 in Patient 8 was the site of microscopic tumor infiltration with fibrous reaction (measurement of the percentage of cancer cells and immunohistochemical study not performed). The lymph node isolated in Patient 3 was small and presented islets of cancer cells not expressing CEA in immunoperoxydase. Finally, the primary tumor in Patient 2 was composed of a mass of colloid and fibrous tissue surrounding the foci of cancer cells.

For these lesions, the tumor-to-blood, tumor-to-muscle and tumor-to-normal lymph node ratios in the biodistribution study were lower than 3, 10 and 5, respectively. However, for tumors with an uptake of more than 20% ID/kg, these same ratios were higher than 10, 20 and 10, respectively. For Patient 7b, whose HAMA existed before anti-CEA/anti-In-DTPA injection, tumor uptake was less than 20% ID/kg (12% and 7% ID/kg). However, the tumor-to-blood and muscle ratios were elevated (>30), whereas the tumor-to-normal lymph node ratio was lower than 10.

DISCUSSION

Our results show the good diagnostic sensitivity of immunoscintigraphy performed with anti-CEA/anti-In-DTPA and ^{111}In-diDTPA-TL for MTC recurrences and the effi-

TABLE 3
Biodistribution and Immunohistochemistry Studies

Patient no.	Tumor Type	Biodistribution %ID/kg	T-to-blood	T-to-mus	T-to-nln	Immunohistochemistry IH	%Cell
1	LyN 1	125	131	291	32.5	++	75
	LyN 2	139	148	322	36	+++	90
2	pt	4.02	1	2.6	3.3	++	50
3	pt	22.3	13.9	41.3	11.3	+	60
	LyN	2.75	1.7	5.1	1.4	−	<1
7b	LyN 1	12.05	55	100	7	+++	30
	LyN 2	6.9	31.4	57	4	++	30
8	LyN 1	37	23	24.8	15	++	90
	LyN 2	4.22	2.7	2.8	1.7	nd	nd

Type = tumor type; LyN = lymph node; pt = primary tumor; mus = muscle; nln = normal lymph node; IH = immunohistochemistry; % cell = percentage of cancer cells in tumor.

ciency of RIGS due to satisfactory tumor-to-normal tissue ratios.

Several studies have shown the capability of immunoscintigraphy performed with ^{131}I- or ^{111}In-labeled anti-CEA monoclonal antibodies to visualize MTC recurrences (*17–23*). However, image interpretation sometimes is difficult after injection of directly radiolabeled anti-CEA antibody because of nonspecific bone marrow, vascular and especially hepatic activity. It requires the use of anatomical landmarks (^{99m}Tc-albumin for the vascular compartment and ^{99m}Tc-HMDP for bone structure) as well as image processing to saturate nonspecific activity (*22*). This methodology complicates the examination and can cause errors for the inexperienced interpreter. For colon cancer, the two-step radioimmunotargeting method provides tumor-to-normal tissue contrasts four to five times better than those obtained with direct labeling of the same antibody (*26*). In our study, whole-body scan images showed the presence of small MTC recurrences, even within the liver or mediastinum, without anatomical landmarks and image processing. In all cases, ECT specified the topography of the lesions visualized in the whole-body scan and never indicated pathological foci not visualized by the whole-body scan.

Anti-CEA/anti-In-DTPA and ^{111}In-diDTPA-TL imaging sensitivity was good, and in two of three patients immunoscintigraphy was the only method to visualize proved recurrences. The presence of HAMA before anti-CEA/anti-In-DTPA injection in one patient caused no clinical intolerance reaction and did not reduce immunoscintigraphy's ability to visualize recurrences. However, immunoscintigraphy was negative in two patients. Although tumor recurrences have not been confirmed in these patients after 6 mo of follow-up, it should probably be considered as false-negative because a rise in baseline TCT concentration after stimulation with pentagastrin, was suggestive of the presence of tumor recurrences. However, the moderate increases in TCT concentration in these two patients would seem indicative of small recurrences. Moreover, some authors have noted a moderate increase in TCT in subjects with no MTC (*27,28*). In our study, immunoscintigraphy was positive for all patients who had a baseline TCT concentration above 200 ng/liter. This possible relationship between TCT concentration and immunoscintigraphic sensitivity requires further investigation. However, there would seem to be no relationship between serum CEA concentration and immunoscintigraphic sensitivity. Only one of five cases in which immunoscintigraphy detected a recurrence showed a significant (22 ng/ml) increase in serum CEA concentration. The specificity of immunoscintigraphy with anti-CEA/anti-In-DTPA and ^{111}In-diDTPA-TL was good since there were no false-positive results.

RIGS was complementary to immunoscintigraphy and detected seven of nine tumor foci. Moreover, in two patients, RIGS enabled the surgeon to excise tumors in involved lymph nodes previously visualized by immunoscintigraphy but were concealed in fibrous tissue growth subsequent to previous surgery. One of the smallest tumor foci (<10 mm in diameter) visualized by immunoscintigraphy and detected by RIGS had high tumor uptake (125% ID/kg) and tumor-to-normal tissue ratios (>30). The same ratios measured by the intraoperative probe were greater than 2. Rockoff et al. (*29*) have shown that the smallest theoretically detectable superficial or nearly superficial tumor (with uptake ratios above 20) is 0.25 cm^2. It is thus not surprising that the intraoperative probe failed to detect lymph nodes with microscopic involvement and low antibody uptake. Thus, negative RIGS would not seem to preclude the practice of systematic neck nodal dissection, particularly for treatment of a primary tumor.

To date, clinical studies of RIGS have generally been carried out with ^{125}I because of the low energy of its gamma radiation (*30–32*). However, the long physical half-life of this radionuclide (60 days) and its high urinary excretion could cause significant radioactive contamination in widespread routine use and ultimately limit its application. For the use of RIGS in clinical practice, a more suitable radionuclide, such as ^{111}In or ^{99m}Tc, is advisable. The main problem concerning the use of these radionuclides is that their gamma radiation energy is relatively

high. The radiation emitted by a nontumor source underlying the tumor (such as blood vessels) cannot be absorbed by the intervening tissues and thus reaches the probe detector. A RIGS feasibility study (*33*) performed on 10 patients with colorectal cancers who were studied using ^{111}In-labeled anti-CEA (F6) monoclonal antibody showed that background activity was too high to obtain tumor-to-normal tissue count ratios above 1.5 (i.e., ratios adequate for tumor detection). Our study indicates that tumor-to-normal tissue ratios above 1.5, and often 2, can be obtained in most cases by the two-step radioimmunotargeting technique, thus enabling RIGS detection of small tumors (<20 mm in diameter).

ACKNOWLEDGMENTS

The authors thank Drs. Du Rostu, Chupin, Beutter, Murat and Bailly and Prof. Bigorgne and Visset for their collaboration, Miss Giacalone for technical assistance, Prof. Charbonnel for advice and Mr. Gray for editorial assistance.

REFERENCES

1. Frank K, Raue F, Lorenz D, Hefarth C, Ziegler R. Importance of ultrasound examination for the follow-up of medullary thyroid carcinoma: Comparison with other localization methods. *Henry Ford Hosp Med J* 1987;35: 122–123.
2. Schwerk WB, Grün R, Wahl R. Ultrasound diagnosis of C-cell carcinoma of the thyroid. *Cancer* 1985;55:624–630.
3. Crow JP, Azar-Kia B, Prinz RA. Recurrent occult medullary thyroid carcinoma detected by MR imaging. *AJR* 1989;152:1255–1256.
4. Baulieu JL, Guilloteau D, Kelisle MJ, et al. Radioiodinated metaiodobenzylguanidine uptake in medullary thyroid cancer. A French cooperative study. *Cancer* 1987;60:2189–2194.
5. Clarke SEM, Lazarus C, Mistry R, Maisey MN. The role of technetium-99m pentavalent DMSA in the management of patients with medullary carcinoma of the thyroid. *Br J Radiol* 1987;60:1089–1092.
6. Talpos GB, Jackson CE, Froelich JW, Kambouris AA, Block MA, Tashjian AH. Localization of residual medullary thyroid cancer by thallium/technetium scintigraphy. *Surgery* 1985;98:1189–1196.
7. Hoefnagel CA, Delprat CC, Zanin D, van der Schoot JB. New radionuclide tracers for the diagnosis and therapy of medullary thyroid carcinoma. *Clin Nucl Med* 1988;13:159–165.
8. Hilditch TE, Connell JMC, Elliott AT, Murray T, Reed NS. Poor results with technetium-99m(V) DMSA and iodine-131 MIBG in the imaging of medullary thyroid carcinoma. *J Nucl Med* 1986;27:1150–1153.
9. Udelsman R, Mojiminiyi OA, Soper NDW, Buley ID, Shepstone BJ, Dudley NE. Medullary carcinoma of the thyroid: management of persistent hypercalcitonaemia utilizing [^{99m}Tc](V)dimercaptosuccinic acid scintigraphy. *Br J Surg* 1989;76:1278–1281.
10. Guerra U, Terzi A, Giubbini R, Bestagno M. The use of ^{99m}Tc(V)DMSA as imaging for the medullary thyroid carcinoma (MTC). *J Nucl Med* 1988;32: 242–247.
11. Samaan NA, Yang KP. Localization of a radiolabeled monoclonal antibody to calcitonin in rat medullary thyroid carcinoma allografts. *Henry Ford Hosp Med J* 1987;35:153–156.
12. Manil L, Boudet F, Motte PH, et al. Positive anticalcitonin immunoscintigraphy in patients with medullary thyroid carcinoma. *Cancer Res* 1989;49: 5480–5485.
13. Guilloteau D, Baulieu JL, Besnard JC. Medullary thyroid carcinoma imaging in an animal model: Use of radiolabeled anticalcitonin F(ab')$_2$ and meta-iodobenzylguanidine. *Eur J Nucl Med* 1985;11:198–200.
14. Delellis RA, Rule AH, Spiler I, Nathanson L, Tashjian AH, Wolfe HJ. Calcitonin and carcinoembryonic antigen as tumor markers in medullary thyroid carcinoma. *AJCP* 1978;70:587–594.
15. Talerman A, Lindeman J, Kievit-Tyson PA, Drögue-Droppert C. Demonstration of calcitonin and carcinoembryonic antigen (CEA) in medullary carcinoma of the thyroid (MCT) by immunoperoxidase technique. *Histopathology* 1979;3:503–510.
16. Economidou J, Karacoulis P, Manousos ON, Manesis E, Kydonakis A, Koutras DA. Carcinoembryonic antigen in thyroid disease. *J Clin Pathol* 1977;30:878–880.
17. Berche C, Mach JP, Lumbroso JD, et al. Tomoscintigraphy for detecting gastrointestinal and medullary thyroid cancers: first clinical results using radiolabeled monoclonal antibodies against carcinoembryonic antigen. *Br Med J* 1982;285:1447–1451.
18. Reiners C, Eilles C, Spiegel W, Becker W, Börner W. Immunoscintigraphy in medullary thyroid cancer using an ^{123}I- or ^{111}In-labelled monoclonal anti-CEA antibody fragment. *J Nucl Med* 1986;25:227–231.
19. Lastoria S, Cavallo PP, Barile V, et al. Selective venous catheterisation, ^{131}I MIBG and ^{111}In-anti-CEA F(ab')$_2$ immunoscintigraphy in the diagnosis of thyroid medullary carcinoma. *J Nucl Med Allied Sci* 1987;31:95.
20. Edington HD, Watson CG, Levine G, et al. Radioimmunoimaging of metastatic medullary carcinoma of the thyroid gland using an indium-111-labeled monoclonal antibody to CEA. *Surgery* 1988;104:1004–1010.
21. Cabezas RC, Berna L, Estorch M, Carrio I, Garcia-Ameijeiras A. Localization of metastases from medullary thyroid carcinoma using different methods. *Henry Ford Hosp Med J* 1989;37:169–172.
22. Vuillez JP, Peltier P, Caravel JP, Chetanneau A, Saccavini JC, Chatal JF. Immunoscintigraphy using ^{111}In-labeled F(ab')$_2$ fragments of anticarcinoembryonic antigen monoclonal antibody for detecting recurrences of medullary thyroid carcinoma. *J Clin Endocrinol Metab* 1992;74:157–163.
23. O'Byrne KJ, Hamilton D, Robinson I, Sweeney E, Freyne PJ, Cullen MJ. Imaging of medullary carcinoma of the thyroid using ^{111}In-labelled anti-CEA monoclonal antibody fragments. *Nucl Med Commun* 1992;13:142–148.
24. Le Doussal JM, Gruaz-Guyon A, Martin M, Gautherot E, Delaage M, Barbet J. Targeting of indium-111-labeled bivalent hapten to human mediated by bispecific monoclonal antibody conjugates: imaging of tumors hosted in nude mice. *Cancer Res* 1990;50:3445–3452.
25. Le Doussal JM, Martin M, Gautherot E, et al. In vitro and in vivo targeting of radiolabeled monovalent and divalent haptens with dual specificity monoclonal antibody conjugates: enhanced divalent hapten affinity for cell-bound antibody conjugate. *J Nucl Med* 1989;30:1358–1366.
26. Barbet J, Chetanneau A, Le Doussal JM, et al. Imaging of primary colorectal carcinoma in humans with In-111-labeled low molecular weight bivalent hapten and dual specificity monoclonal antibody conjugate [Abstract]. *J Nucl Med* 1991;32:940.
27. Body JJ, Health H III. "Nonspecific" increases in plasma immunoreactive calcitonin in healthy individuals: discrimination from medullary thyroid carcinoma by a new extraction technique. *Clin Chem* 1984;30:511–514.
28. Kempter B, Ritter MM. Unexpected high calcitonin concentrations after pentagastrin stimulation. *Clin Chem* 1991;37:473–474.
29. Rockoff SD, Goodenough DJ, McIntire R. Theoretical limitations in the immunodiagnostic imaging of cancer with computed tomography and nuclear scanning. *Cancer Res* 1980;40:3054–3058.
30. Martin EW, Mojzisik CM, Hinkle GH, et al. Radioimmunoguided surgery using monoclonal antibody. *Am J Surg* 1988;156:386–392.
31. Neiroda C, Mojzisik CM, Sardi A, et al. Staging of carcinoma of the breast using a hand-held gamma detecting probe and monoclonal antibody 72.3. *Surg Gynecol Obstet* 1989;124:56–59.
32. Sardi A, Workman M, Mojzisik CM, Hinkle GH, Neiroda C, Martin EW. Intraabdominal recurrence of colorectal cancer detected by radioimmunoguided surgery (RIGS) system. *Arch Surg* 1989;124:56–59.
33. Curtet C, Vuillez JP, Daniel G, et al. Feasibility of radioimmunoguided surgery of colorectal carcinomas using indium-111 CEA-specific monoclonal antibody. *Eur J Nucl Med* 1990;17:299–304.